Journal of Solid State Chemistry **152,** 57–67 (2000)
doi:10.1006/jssc.2000.8669, available online at http://www.idealibrary.com on IDEAL®

Controlling Growth of Novel Solid-State Materials via Discrete Molybdenum-Oxide-Based Building Blocks as Synthons

Leroy Cronin, Paul Kögerler, and Achim Müller[1]

Fakultät für Chemie, Universität Bielefeld, Postfach 100131, 33501 Bielefeld, Germany

The understanding of the fundamental principles behind the growth of materials from discrete molecules to new solid-state materials is presently a great challenge. Herein novel nanoscale polyoxometalate clusters with circular and spherical topologies are described and examples that have application in the study of molecular growth processes are highlighted. This is because it is now possible to control the formation of solid-state structures from certain types of polyoxometalate fragments that can be described as synthon-based building blocks. This ability, combined with the enormous number of ways that these building blocks can be linked together, is opening completely new and fascinating avenues for the synthesis of solid-state structures with predesigned properties. © 2000 Academic Press

Key Words: **polyoxometalates; molecular growth; designed solid-state structures; synthon-based building blocks.**

1. INTRODUCTION

The deliberate synthesis of multifunctional compounds and materials with synthon-based building blocks (the term "synthon" seems justified for reactive polyoxometalate fragments/building blocks which can be easily generated and linked) is one of the most challenging problems in contemporary chemistry. Pertinent targets include the synthesis of materials with network structures that have desirable and predictable properties, such as mesoporosity (1) (due to well-defined cavities and channels), electronic and ionic transport (2), ferro- as well as ferrielasticity, luminescence and catalytic activity (3,4). The synthesis of such compounds or solids from preorganized linkable building blocks with well-defined geometries and chemical properties is, therefore, of special interest (5). In this article, we will focus on the relationship between some polyoxometalate-based giant clusters and solid-state structures derived from these precursors. Accordingly, a strategy will be presented that allows the *intentional* synthesis of solid-state materials, both by designing and utilizing known clusters that can be treated as synthon-based building blocks (and thus these synthons can be linked together), with preferred structure and function.

[1]To whom correspondence should be addressed. E-mail: a.mueller@uni-bielefeld.de.

2. BASIC BUILDING BLOCKS AND STRUCTURAL TYPES IN MOLYBDENUM-BASED POLYOXOMETALATE CLUSTERS

In generating large complex molecular systems it has to be realized that the directed and nondirected linking of a huge variety of basic and well-defined fragments affects many natural processes. An impressive example of this, discussed in virtually all textbooks on biochemistry, is the self-aggregation process of the tobacco mosaic virus, which is based on preorganized units (6). This process exemplifies the strategy used by nature in controlling the linking of fragments to form larger units and linking the latter again, see Fig. 1.

To copy nature's approach in the construction of metal-oxide-based clusters, relatively large molecular fragments must be functionalized with groups that allow linking through characteristic reactions. For example, the protonation of highly reactive $\{(\mu\text{-}O_3)\text{–}MoO_3\}$ (so-called "anti-Lipscomb" units) groups positioned on polyoxometalate cluster fragments results in condensation reactions of the fragment under H_2O formation (7). In the case of the generation of large polyoxometalate clusters (8, 9), the above-mentioned concept of preorganized units is of particular importance due to the fact that *differently transferable building units* govern the structural chemistry.

2.1. *Transferable Building Units in* $\{Mo_{36}\}/\{Mo_{57}\}$ *and the* $\{Mo_{154}\}/\{Mo_{176}\}$ *"Giant-Wheel" Clusters*

From a fundamental point of view the construction and linking of polyoxometalate clusters containing repeating units, which can be considered as synthon-based building blocks, is conceptually very powerful, both in the mental

0022-4596/00 $35.00
Copyright © 2000 by Academic Press
All rights of reproduction in any form reserved.

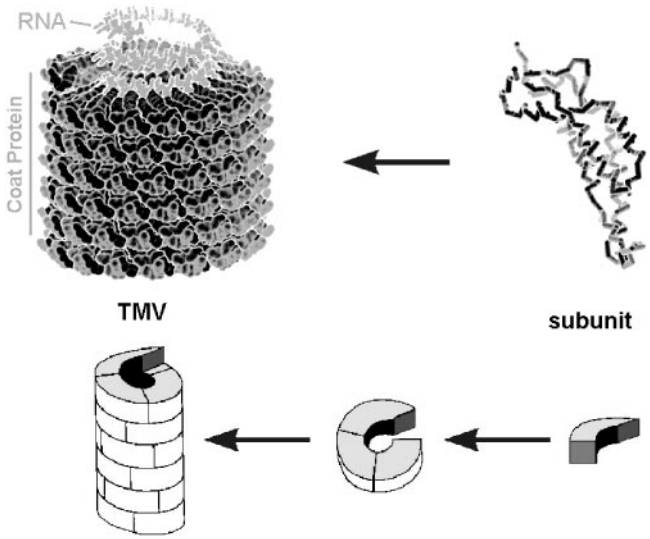

FIG. 1. General scheme depicting the assembly procedure of the tobacco mosaic virus with nature's self-assembly approach.

decomposition and construction of real clusters containing thousands of atoms. For instance, building blocks containing 17 molybdenum atoms ($\{Mo_{17}\}$ units) can be given as an example of a generally repeated building block or synthon which can be considered to form anions consisting of two or three of these units. The resulting species are of the $\{Mo_{36}\}$ type (e.g., $[(MoO_2)_2\{H_{12}Mo_{17}(NO)_2O_{58}(H_2O)_2\}]^{12-}$, a two-fragment cluster $\equiv \{Mo'_1\}_2\{Mo_{17}\}_2$) or of the $\{Mo_{57}\}$ type (e.g. $[(VO(H_2O))_6(Mo_2(H_2O)_2(OH))_3\{Mo_{17}(NO)_2O_{58}(H_2O)_2\}_3]^{21-}$, a three-fragment cluster $\equiv \{V\}_6\{Mo'_2\}_3\{Mo_{17}\}_3$) (10–12). The latter can be obtained from the former cluster under reducing conditions in the presence of the relatively strong nucleophilic linker V^{IV}, see Fig. 2.

It has now been well established that a solution containing $\{Mo_{17}\}$-type species can be reduced and acidified further to yield a mixed-valence wheel-shaped cluster (and derivatives thereof) $\{Mo_{154}\} \equiv [Mo_{154}(NO)_{14}O_{434}(OH)_{14}(H_2O)_{70}]^{28-}$ (13). Formally, this cluster can be regarded as a tetradecamer with D_{7d} symmetry (if the hydrogen atoms are excluded) and structurally generated by linking 140 MoO_6 octahedra and 14 $MoO_6(NO)$ pentagonal bipyramids (Fig. 3).

Using the general architecture principle for the "giant-wheel"-type clusters the structural building blocks, e.g., for the $\{Mo_{154}\}$-type cluster, can be deduced and expressed in terms of the three different building blocks as $[\{Mo_2\}_n\{Mo_8\}_n\{Mo_1\}_n]^{n-}$ ($n = 14$). The building blocks of the type $\{Mo_8\}$, $\{Mo_2\}$, and $\{Mo_1\}$ are each present 14 times in the original cluster and the corresponding analogous (synthesized without the NO ligands) iso-

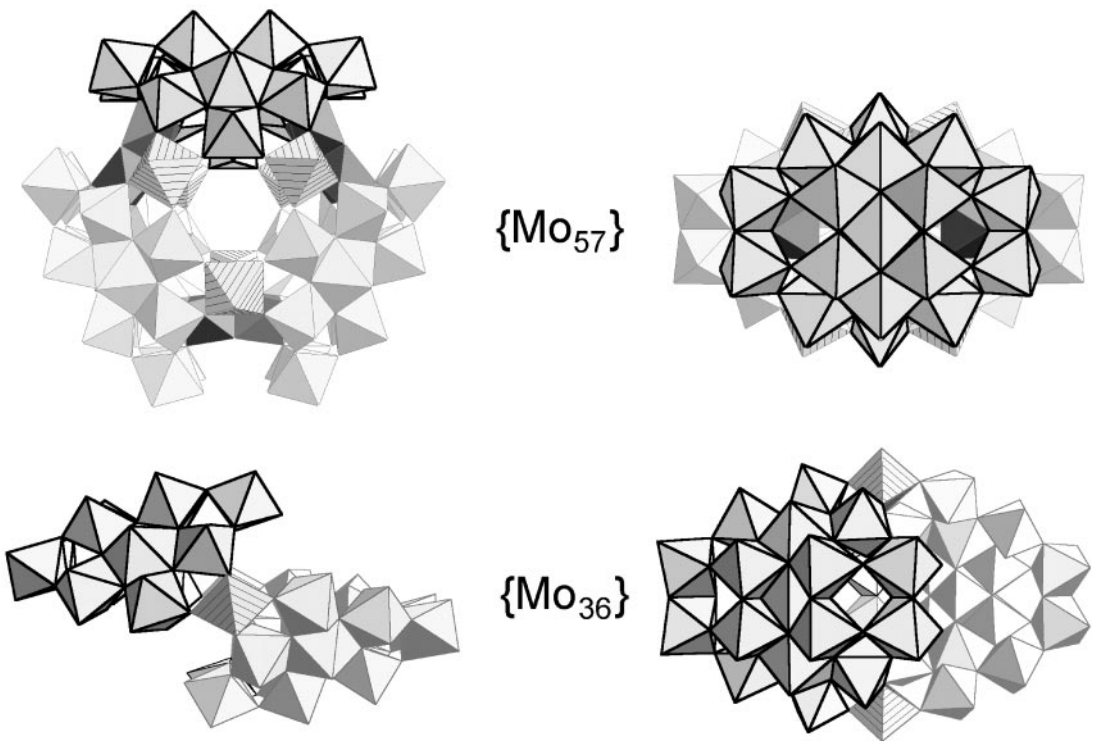

FIG. 2. Polyhedral representations of the $\{Mo_{36}\}$ and $\{Mo_{57}\}$ clusters (top and side views). One $\{Mo_8\}$ group is highlighted in each view with a black outline.

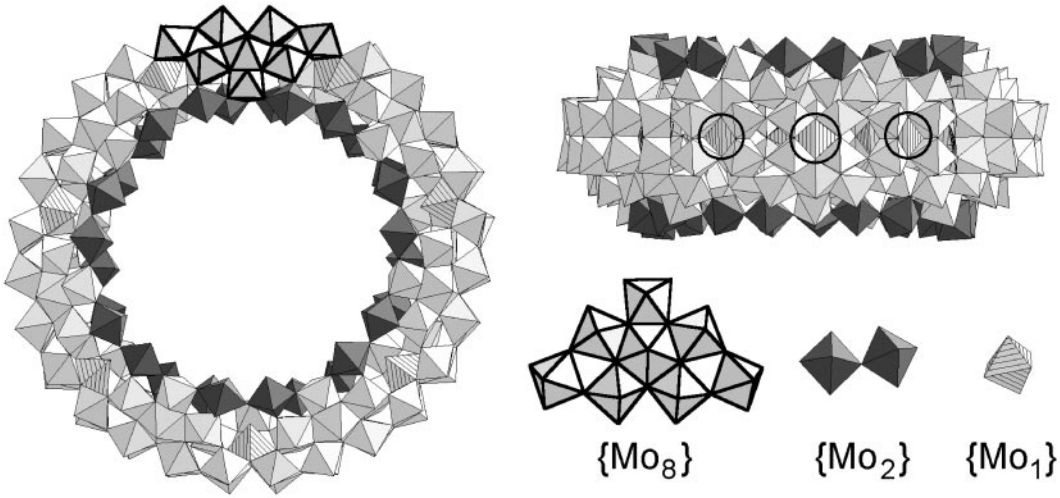

FIG. 3. Representation showing the general architecture principle for the "giant-wheel"-type clusters, using the $\{Mo_{154}\}$ cluster (top view, left-hand side, and side view, right-hand side) as an example. The structural building blocks for all the "giant-wheel" clusters can be formulated as comprising $\{Mo_8\}$ units that are connected together *via* the $\{Mo_2\}$ units on the inner side of the wheel. Finally, the $\{Mo_1\}$ units form the equatorial plane of the ring linking the $\{Mo_8\}$ units together above and below the equator (the $\{Mo_1\}$ units are circled in the side view of the cluster for clarity).

polyoxometalate cluster $[Mo_{154}O_{448}(OH)_{14}(H_2O)_{70}]^{14-}$ (having 14 $\{MoO\}^{4+}$ instead of 14 $\{MoNO\}^{3+}$ groups) which turned out to comprise one prototype of the soluble amorphous molybdenum blue species (14). Furthermore, a larger $\{Mo_{176}\}$ "giant-wheel" cluster with D_{8h} symmetry can also be synthesized under similar conditions; the larger cluster geometrically results if two more of each of the three different types of building units are added to the "giant-wheel" $\{Mo_{154}\}$ cluster (15). This presents a hexadecameric ring structure, containing 16 ($n = 16$) instead of 14 of each of the three aforementioned building blocks (Fig. 4) (cf. (22)).

This result is interesting from the point of view that it is possible to express the architecture of these systems with a type of Aufbau principle. Furthermore, the $\{Mo_{17}\}$ unit, with C_{2v} symmetry, can be subdivided again into one $\{Mo_1^*\}$ and two $\{Mo_8\}$ units (two $\{Mo_8\}$-type groups linked by an $\{Mo_1^*\}$-type unit). It is interesting to note that the $\{Mo_8\}$ building blocks are found in many other large poly-

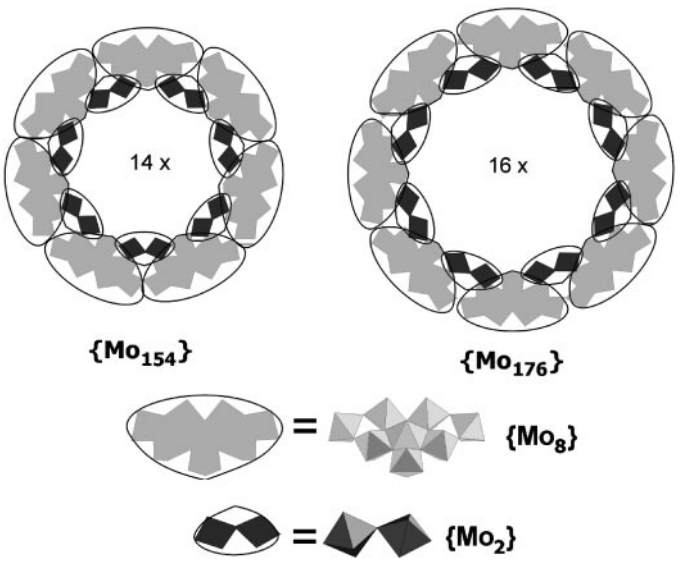

FIG. 4. Representation of the upper halves of the tetradecameric $\{Mo_{154}\}$ and the hexadecameric $\{Mo_{176}\}$ "giant-wheel" clusters. The $\{Mo_8\}$ and $\{Mo_2\}$ building blocks are shown below. The equatorial $\{Mo_1\}$ building blocks, which connect the two halves of the "Giant-Wheels" together, are not visible in this representation.

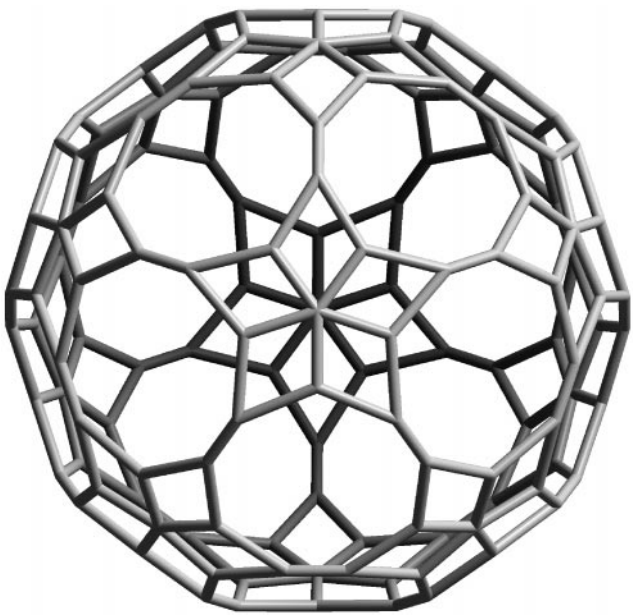

FIG. 5. Wire frame representation showing how all the metal atoms of the $\{Mo_{132}\}$ Keplerate are connected.

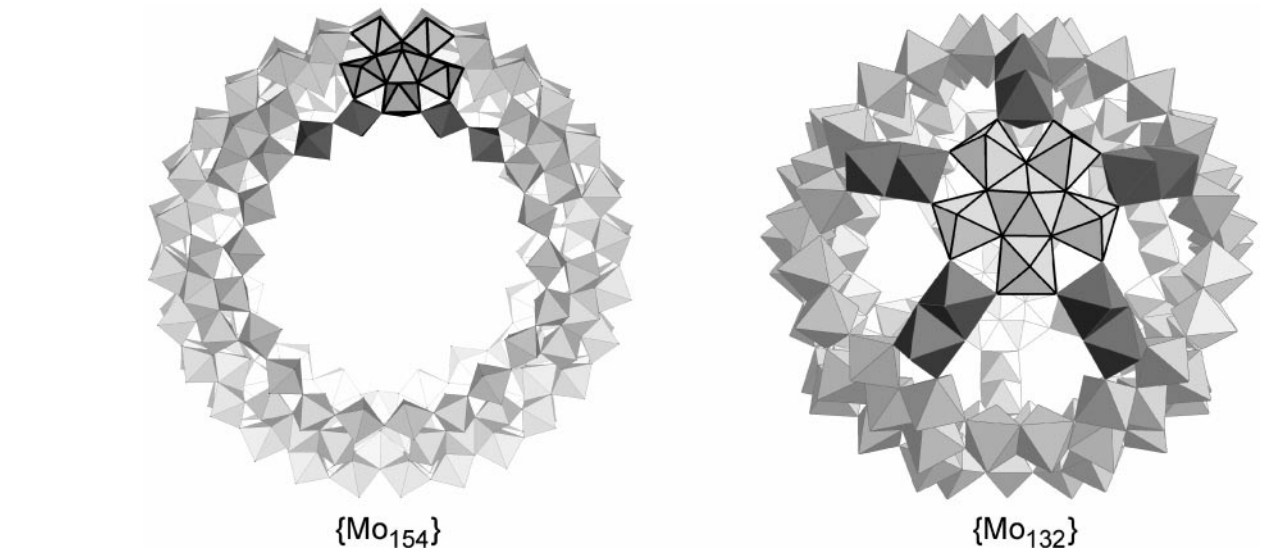

FIG. 6. Comparison of the polyhedral representations of the $\{Mo_{132}\}$ Keplerate with the $\{Mo_{154}\}$ cluster (not to scale) with the pentagonal $\{Mo(Mo)_5\}$ (in thick lines) and the adjoining $\{Mo_2\}$ (dark gray) units emphasized in each. It is important to know, in the context of synthesis, that the $\{Mo_2\}$ units have a different structure in each class of cluster, but it is only these units which have been observed to be exchangeable for other metal ions.

oxometalate structures and $\{Mo_8\}$ itself can be divided into a (close-packed) $\{Mo(Mo)_5\}$ pentagon built up by a central MoO_7 pentagonal bipyramid sharing edges with five MoO_6 octahedra and two more MoO_6 octahedra sharing corners with atoms of the pentagon (Fig. 3). Additionally, the surfaces of the "giant-wheel" clusters can be modified by ligand-exchange reactions (16).

2.2. *Transferable Building Units in Spherical Keplerate Clusters* $(Pentagon)_{12}$ $(Linker)_{30}$

One of the most striking examples from polyoxometalate chemistry, showing the enormous number of ways that polyoxometalate fragments can link together, is demonstrated by the spherical inorganic cluster-based Keplerate systems (17–20). For example, one of the spherical clusters of this type reported has the formula $[Mo^{VI}_{72}Mo^{V}_{60}O_{372}(MeCO_2)_{30}(H_2O)_{72}]^{42-}$ ($\{Mo_{132}\}$) and consists of two types of building blocks (Fig. 5): 12 pentagonal $\{Mo(Mo)_5\}$ units and 30 linking $\{Mo^{V}_2\}$ units (this type of $\{Mo_2\}$ unit can be formulated as $\{Mo^{V}_2O_4(OOR)^+\}$ ($R = CCH_3$, CH, PO_2)). In geometrical terms this type of cluster can be described as $(pentagon)_{12}(linker)_{30}$; pentagon = $\{Mo(Mo)_5\}$ and linker = $\{M^{V}_2O_4(OOR)^+\}$, $\{OMo(H_2O)\}^{3+}$, or $\{Fe(H_2O)_2\}^{3+}$.

It is interesting that the $\{Mo^{V}_2\}$ building unit can be formed only in the presence of stabilizing bidentate ligands and it is these units that are able to direct the formation of the $\{(Mo)(Mo)_5\}$ pentagon, which does not exist as an independent unit. Furthermore, the $\{(Mo)(Mo)_5\}$ pentagon found in the Keplerate can be considered to be similar to the $\{(Mo)(Mo)_5\}$ pentagons found in the $\{Mo_8\}$ units, of which the $\{Mo_{57}\}$ and "giant wheel" clusters are comprised, Fig. 6 (20).

3. PROPERTIES OF THE "GIANT-WHEEL" AND KEPLERATE CLUSTERS

Before the construction of solid-state materials with $\{Mo_{154}\} = \{Mo_8\}_n\{Mo_2\}_n\{Mo_1\}_n$ ($n = 14$ or 16) and $\{Mo_{132}\} = (pentagon)_{12}(linker)_{30}$-type precursors is discussed it is instructive to consider the properties unique

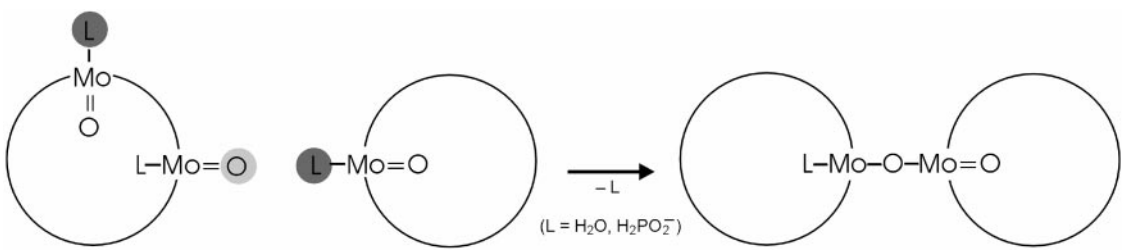

FIG. 7. Schematic representation of the basic assembly principle of the "giant-wheel"-shaped cluster units forming the networks and layers. The formation is based on the synergetically induced functional complementarity of the $\{Mo_2\}$ units O=Mo(*L*) (e.g., $L = H_2O$, $H_2PO_2^-$) on their surfaces.

to these clusters. In this manner it should be possible to build on these properties and develop strategies to fine-tune the overall properties of the new material. Interesting and useful properties of the discrete clusters include the following:

- The "giant-wheel" clusters exhibit a nanometer-sized cavity, presenting new perspectives for novel host–guest chemistry according to the different sites on the cluster surfaces.
- The Keplerate clusters have a nanometer-sized cavity that presents the possibility to completely encapsulate a guest within the cluster.
- The "giant-wheel" clusters have an extended hydrophilic inner and outer surface due to the presence of $5n$ H_2O ligands ($2n$ H_2O ligands belong to the $\{Mo_2\}$ and $3n$ H_2O ligands to the $\{Mo_8\}$ groups).
- The molybdenum-oxide-based clusters render a molecular model for catalytically active metal-oxides of industrial importance.
- The periphery of the clusters (both the "giant-wheel" and Keplerate clusters) have high electron density; this has implications for the activation of small molecules coordinated to the surface site.
- The "giant-wheel" clusters support n electronically uncoupled $\{Mo_5O_6\}$ compartments of incomplete double-cubane type, each of which carries two delocalized $4d$ electrons, a situation which is comparable to a so-called electronic necklace corresponding to an electron-storage system where the uncoupled storage elements are threaded like pearls on a string. These compartment-delocalized electrons are responsible for the intense blue color (21, 22).
- It is possible to generate deliberately discrete and well-defined structural defects on the inner surface of the cluster ring by abstracting positively charged $\{Mo_2\}$ groups using special ligands, which have a high affinity to these groups (see below). This drastically changes both the reactivity and the shape (23).
- It is possible to selectively replace the $\{Mo_2\}$ groups on the ring ($\{Mo_2\}$) and the $\{Mo_2^V\}$ found in the Keplerate-type clusters with other, high-spin metal centers, e.g., Fe^{3+} ions, respectively (24).
- It is possible to place molecules or replace ligands, e.g., H_2O by CH_3OH (16), at different sites of the surface of the "giant-wheel" clusters, in particular to replace up to two H_2O ligands at the $\{Mo_8\}$ groups (thereby changing the properties of the clusters) and to study direct reactions between the molecules placed inside the cavity.

By the designed synthesis of solid-state structures incorporating such clusters it should be possible to exploit and control these properties and even predict the emergence of new properties that could arise due to the complexity and the size of the systems synthesized.

4. FROM CLUSTERS TO SOLID-STATE STRUCTURES

4.1. Crystal Engineering I: The Linking of "Giant-Wheel" and $\{Mo_{36}\}$ Cluster Synthons to Network Structures

One extremely interesting observation is that it is possible to obtain "giant-wheel"-type species, which are structurally incomplete, comprising defects when compared to the original $\{Mo_{154}\}$ cluster. These defects manifest themselves as

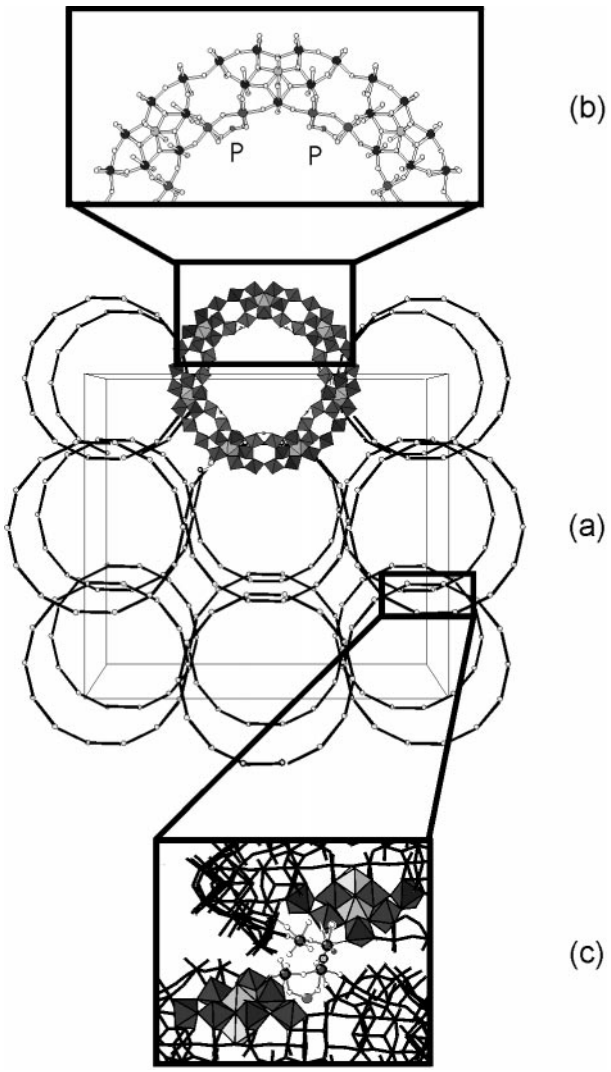

FIG. 8. (a) Perspective view of the framework of $Na_{21}[Mo_{154}O_{462}H_{14}(H_2O)_{54}(H_2PO_2)_7]\cdot$ca. $300\,H_2O$ along the crystallographic c axis, showing the abundance of nanotubes and cavities. For clarity, only one complete ring (without the P ligands) is shown in polyhedral representation. With respect to the other rings, only the centers of the $\{Mo_1\}$ units are given and connected. (b) Ball-and-stick representation of the upper half of a ring segment showing the principal positions of the $H_2PO_2^-$ ligands. (c) Detailed view [perpendicular to (a) and (b)] of the bridging region between two cluster rings emphasizing one $\{Mo_8\}$ and one $\{Mo_1\}$ unit (in polyhedral representation) as well as one $\{Mo_2\}^{2+}$ unit and one $H_2PO_2^-$ ligand (in ball-and-stick representation).

missing $\{Mo_2\}^{2+}$ units, but statistically these defects can sometimes be seen as underoccupied $\{Mo_2\}^{2+}$ units when the distribution is affected by rotational or translational disorder within the crystal structure (27). When wheel clusters with defects are considered the numbers of each type of building block are not identical as a fraction of the $\{Mo_2\}^{2+}$ groups have been removed. As a result the overall negative charge on the "giant-wheel" increases by two for each of the removed $\{Mo_2\}^{2+}$ groups. These compounds also can be expressed in terms of the "giant-wheel" architecture, with the general formula $[\{Mo_2\}_{n-x}\{Mo_8\}_n\{Mo_1\}_n]^{[n+2x]-}$ where the value x corresponds to the number of defects introduced into the system (in the case of the "giant-wheel" structures, only structures that have $n = 14$ have been discovered with defects to date).

In the case of the $\{Mo_{154}\}$-type cluster, the nucleophilicity at special sites can be increased by either removing several positively charged $\{Mo_2\}^{2+}$ groups with bidentate ligands like formate (that means via formation of defects) (26), or placing electron-donating ligands like $H_2PO_2^-$ on the inner ring surfaces (27) (Figs. 7, 8). This leads to a linkage of the ring-shaped clusters via Mo–O–Mo bonds to form compounds with layers or chains (derived from $\{Mo_{144}\}$ ring units (28)) (Fig. 9) according to a type of crystal engineering (see below). Single crystals of the chain-type compound exhibit interesting anisotropic electronic properties that represent promising fields for further research.

In compounds of that type channels are present, the inner surfaces of which have basic properties in contrast to the acidic channels in zeolites (21). The layer compound can take up small organic molecules such as formic acid, which according to the basicity are partly deprotonated. The reduction of an aqueous solution of sodium molybdate by hypophosphorus (phosphinic) acid at low pH values (≈ 1)

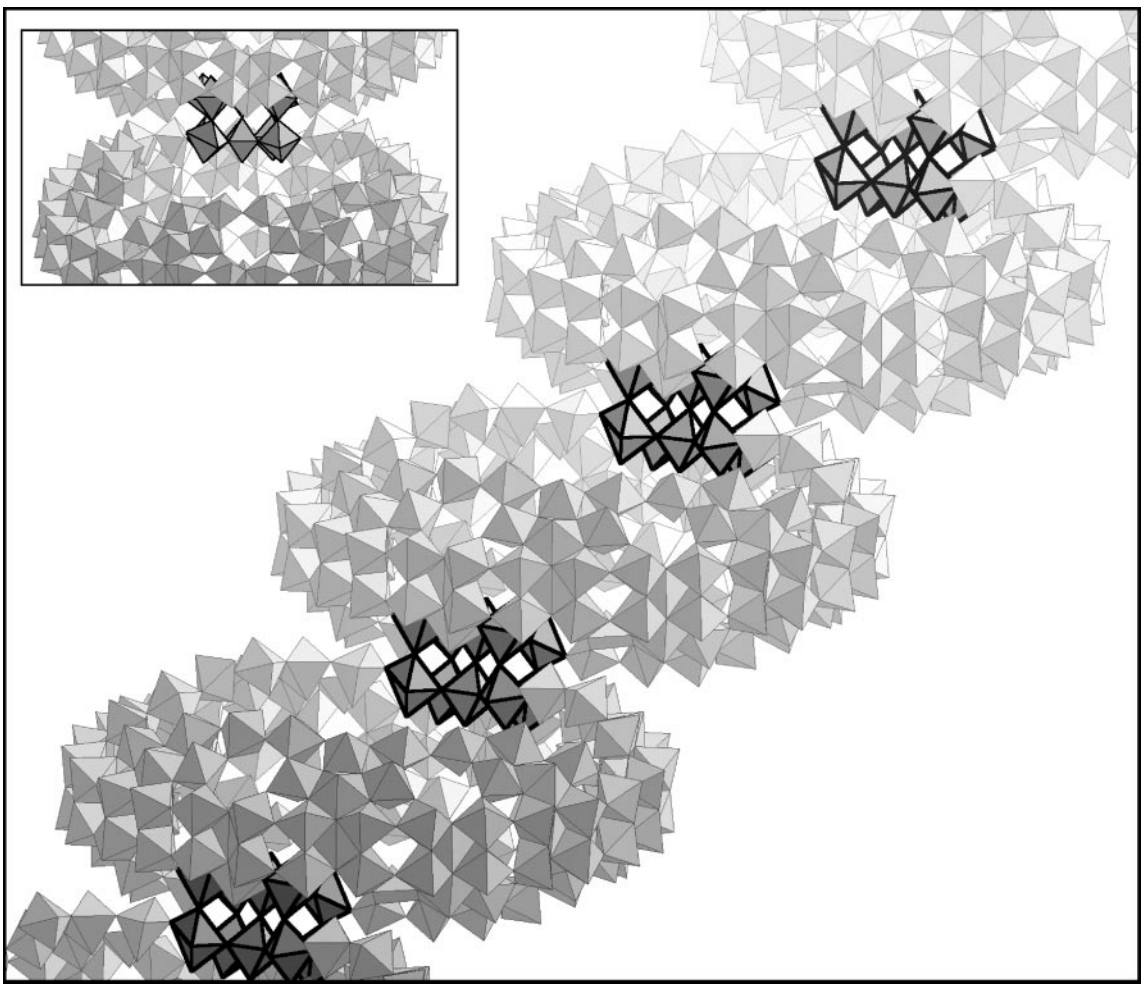

FIG. 9. Polyhedral representation of $\{Mo_{144}\}$ units linked to chains. The linking occurs via the $\{Mo_2\}$ units—the polyhedra formed by the linked $\{Mo_2\}$ units are shown in a black outline. A face-on representation of one of the linking units with a ring above and below the linked polyhedra (also highlighted with a black outline) is shown in the upper left corner for clarity.

results in the formation of nanosized ring-shaped cluster units (defined above) which assemble to form layers of the compound $Na_{21}[Mo_{154}O_{462}H_{14}(H_2O)_{54}(H_2PO_2)_7]\cdot$ ca. 300 H_2O (27). The assembly is based on the synergetically induced complementarity of amphiphilic $\{Mo_2\}$-type $O{=}Mo(H_2O)$ groups and corresponds to the replacement of H_2O ligands of rings by related terminal oxo groups of the $\{Mo_2\}$-type $O{=}Mo(H_2O)$ units of other rings acting formally as ligands (and vice versa). The increased nucleophilicity of the $O{=}Mo$ groups at the ring is induced by coordinated $H_2PO_2^-$ ligands (Fig. 8).

This type of linking is not confined to the larger clusters; previously it has been shown that the smaller $\{Mo_{36}\}$ clusters (formally these are generated by the linking of two $\{Mo_{17}\}$ units with two $\{Mo_1\}$ units) can be linked together into 1-D polymers by the incorporation of $\{Mo_2O_4(\mu\text{-}O)(H_2O)_2\}$ linker groups (29). In a recent study this has been extended by the incorporation of lanthanide ions into the structure which results in the formation of a 1-D-type polymer while linking occurs via an Mo–O–Ln unit; furthermore, two weakly bound electrophilic $\{MoO\}^{3+}$ groups are believed to exist (30).

4.2. *Crystal Engineering II*: *Linking Molecular Keplerate Clusters to Layers*

The solid-state chemistry based on the spherically shaped Keplerate clusters is versatile. In crystals of the $\{Mo_{132}\}$-type species (space group $Fm\bar{3}$), the spheres are ordered according to the cubic close packing scheme (17). This

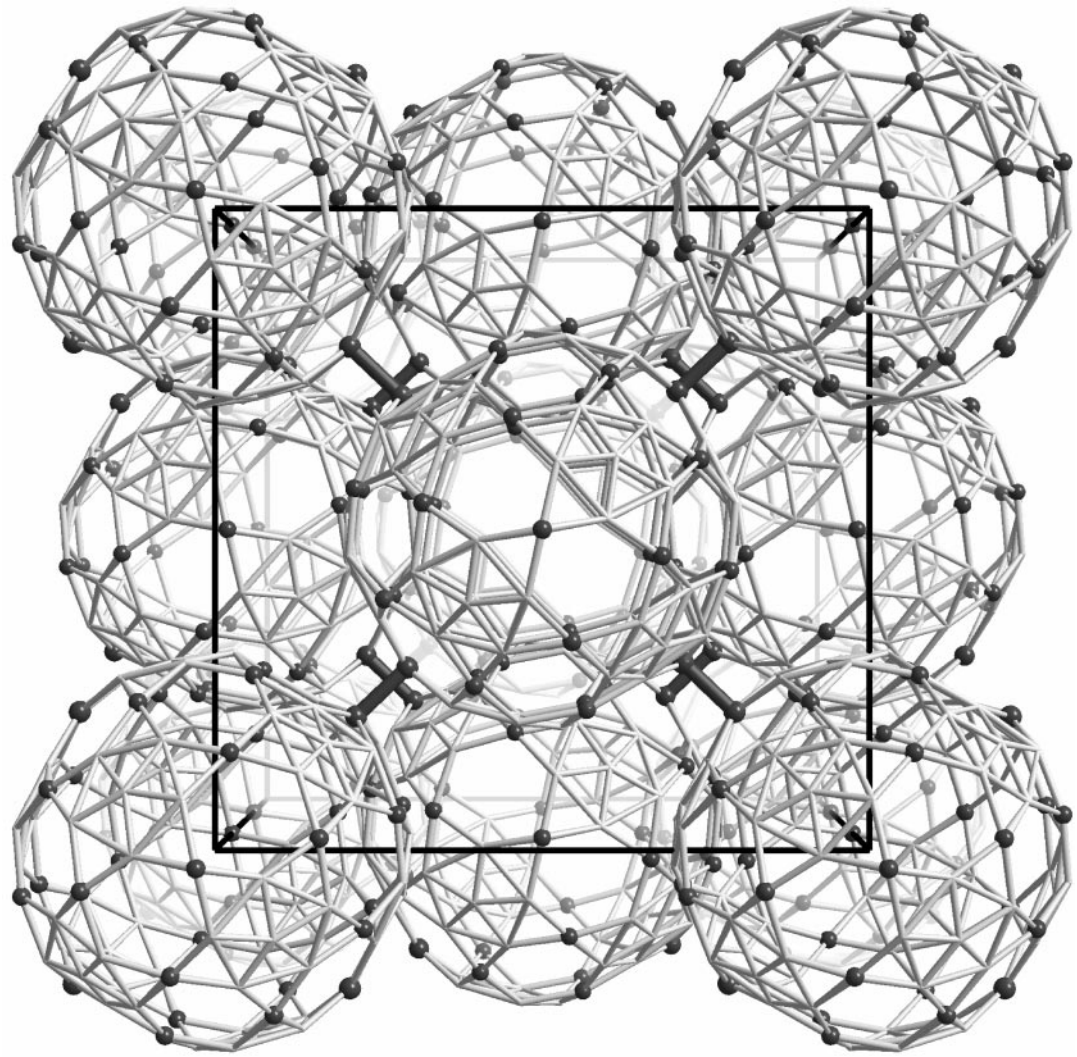

FIG. 10. Wire frame representation of the layer structure of linked $\{Mo_{72}Fe_{30}\}$ units with emphasized Fe–O–Fe bridges along the *a* axis (only the metal atoms are shown; Fe centers, black spheres). The unit cell is also depicted, showing the approximate face-centred cubic packing of the cluster spheres.

packing, similar to that of hard spheres, is simply due to the spherical shape of the cluster's van der Waals surface. In contrast, in the case of a monoclinic crystal modification of the functionalized Keplerate system $\{Mo_{72}Fe_{30}\}$ (19), distinct solid-state reactions, i.e., the linking of these icosahedral spherical clusters to layers, can take place even at room temperature, Fig. 10. During the dehydration process of crystals comprising $\{Mo_{72}Fe_{30}\}$ units, crystal water molecules are expelled in a first (slow) step and the cluster shells approach each other until a minimum distance between the $Fe–OH_2 \cdots H_2O–Fe$ groups (on adjacent clusters) is reached (Fig. 11). This first step is followed by a second (faster) one in which a condensation reaction takes place at four Fe sites on each cluster unit. This reaction mechanism is known for the formation of inorganic polycations at low activation energies:

$$\cdots Fe(H_2O) + (H_2O)Fe \cdots \xrightarrow[\text{dehydration}]{-H^+} \cdots Fe(OH_2) + (HO)Fe \cdots \xrightarrow{-H^+/-H_2O} \cdots Fe–O–Fe \cdots . \quad [1]$$

This reaction finally results in a two-dimensional grid structure found in the compound $[H_4Mo_{72}Fe_{30}O_{254}(CH_3COO)_{10}\{Mo_2O_7(H_2O)\}\{H_2Mo_2O_8(H_2O)\}_3(H_2O)_{87}] \cdot$ ca. 80 H_2O. The four Fe–O–Fe links (Fe–Fe = 3.79 Å) interconnect each cluster unit with four neighboring shells. This also leads to a decrease of the effective magnetic moment from nearly 30 uncoupled Fe(III) centers to approximately 26 uncoupled Fe(III) centers as the iron centers of the (nearly linear) Fe–O–Fe groups are strongly coupled. This situation is typical for structurally similar (linear) $(\mu\text{-O})Fe_2$ complexes.

It is possible to isolate the intermediate compound containing the spherical clusters as discrete entities: $[Mo_{72}Fe_{30}O_{252}(CH_3COO)_{10}\{Mo_2O_7(H_2O)\}\{H_2Mo_2O_8(H_2O)\}_3(H_2O)_{91}] \cdot$ ca. 100 H_2O (Fe–Fe = 5.35 Å) that crystallizes in the same space group ($P2_1/n$) as the freshly prepared precipitated compound, before the dehydration (drying) process. In this compound the short Fe … Fe distances are stabilized by hydrogen bonds ($Fe–OH_2 \cdots OH_2–Fe$ 2.77 Å), see Fig. 11.

In addition, the tiling of icosahedral units in a two-dimensional grid in principle conflicts with classical crystallography, which excludes the presence of C_5 axes. In the layer compound, which crystallizes in the space group *Cmca*, the symmetry is broken by the linking of the icosahedral units via oxygen atoms, thus enabling the arrangement in a two-dimensional grid.

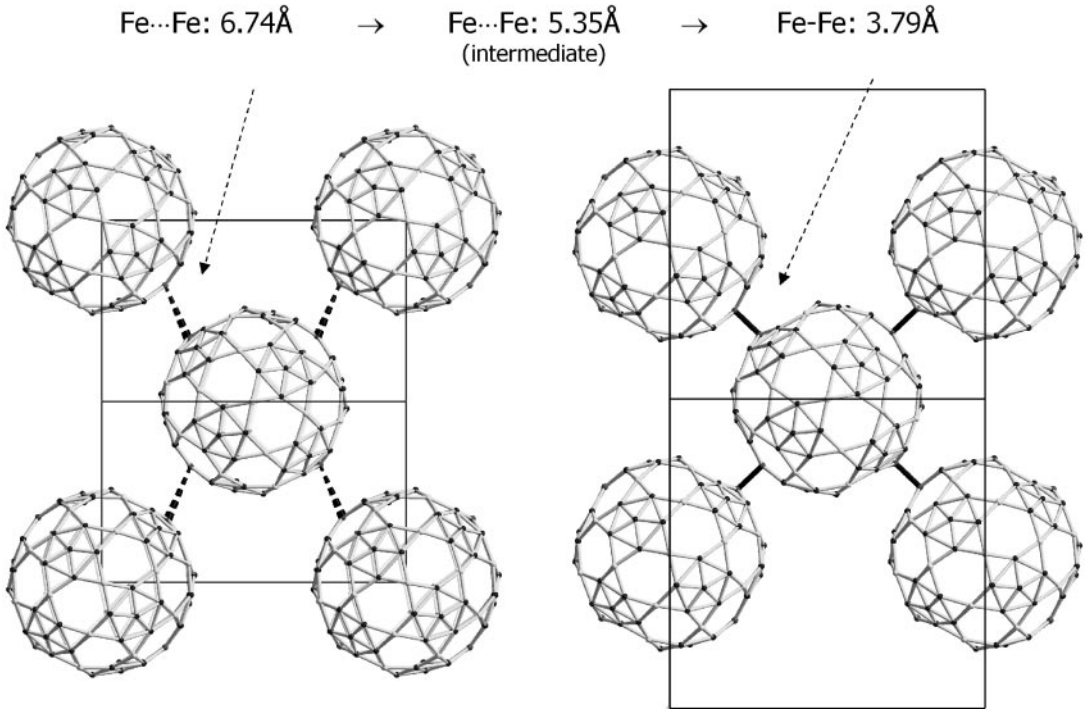

FIG. 11. Representation of the metal skeletons of the cluster units in the $\{Mo_{72}Fe_{30}\}$ layer compound with emphasized links (right side). The condensation reaction proceeds from discrete cluster units (as present in freshly prepared monoclinic crystals of $\{Mo_{72}Fe_{30}\}$; left side) via an intermediate, in which discrete units are approached to each other reaching a minimum distance. This geometry is stabilized by hydrogen bonds between $Fe–OH_2 \cdots H_2O–Fe$ groups which finally react to form the Fe–O–Fe linkers. (A. Müller *et al.*, *Angew. Chem. Int. Ed.* **39,** 1616 (2000)).

5. A MODEL FOR A NUCLEATION AND A LIMITED GROWTH PROCESS: SECTIONS OF SOLID-STATE STRUCTURES INSIDE THE CAVITIES OF MOLECULAR CLUSTERS

It is instructive, when describing or analyzing a solid-state structure, to follow a reductionist approach insofar as the system is mentally reduced into elementary building blocks (e.g., polygons, polyhedra, or aggregates of these) and then the local matching rules are explored according to which the building blocks are assembled to yield the structure under study. A good model system for this procedure is given below. A new type of growth (nucleation) process within the cavity of the above-mentioned molecular $\{Mo_{176}\}$ cluster (which acts here as a compartment) has been observed, resulting in an $\{Mo_{248}\}$-type cluster (31) (see also (32)). This $\{Mo_{248}\}$ cluster consists of an $\{Mo_{176}\}$-type cluster ring, where the ring openings are covered by two $\{36Mo\}$ $(=\{Mo_{36}(H_2O)_{24}O_{96}\})$ fragments, which can be assigned to two hubcaps (these should not be confused with the $[Mo_{36}O_{112}(H_2O)_{16}]^{8-}$ ($\{Mo_{36}\}$) cluster) (Fig. 12). It is important in this context to consider the factors surrounding the nucleation and growth processes that occur: (1) that the subunits within the hubcaps are similar (some are even identical) to those on the $\{Mo_{176}\}$-type cluster and (2) that these $\{36Mo\}$ fragments consist of sections found in the solid-state structure of Mo_5O_{14}. The comparison between relevant parts of the $\{Mo_{248}\}$ cluster and the solid-state structure Mo_5O_{14} (33) reveals surprising parallels (Fig. 13): the hubcaps (if the H atoms of the H_2O ligands are excluded) are nearly identical (the only difference concerns the geometry of the $\{Mo_8\}$ units, of which there are two structural types but only one of these is present in the Mo_5O_{14}) to a section of the crystal lattice of Mo_5O_{14}. Nevertheless, detailed pathways for the initial growth (nucleation) steps of inorganic solid-state structures were unprecedented until now.

6. CONCLUSIONS AND PERSPECTIVES

In order to investigate the border region between the molecular and the macroscopic world, several questions arise, for instance, whether the size of such cluster systems described here has a limit or can we fabricate ever larger

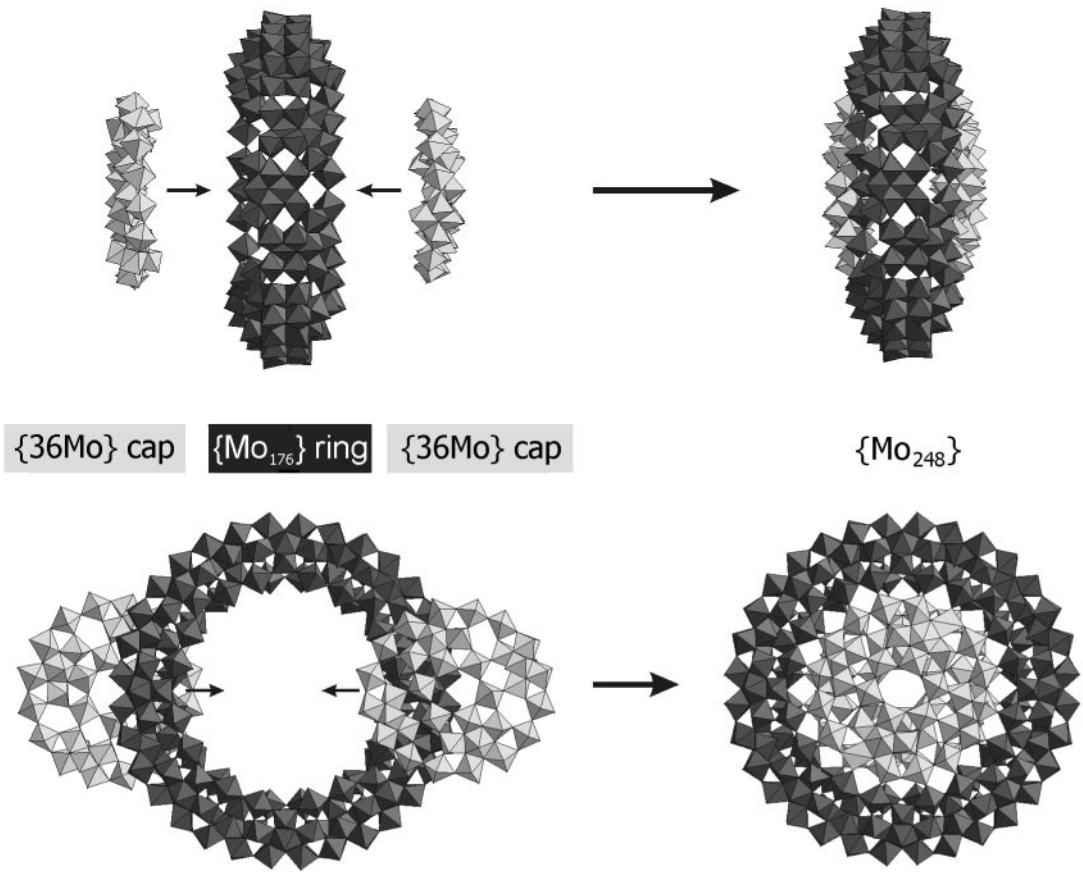

FIG. 12. Schematic representation of the growth process $\{Mo_{176}\} \rightarrow \{Mo_{248}\}$. The structure of one $\{Mo_{248}\}$ cluster can formally be decomposed into one $\{Mo_{176}\}$ ring and two $\{Mo_{36}O_{96}(H_2O)_{24}\}$ "hubcaps".

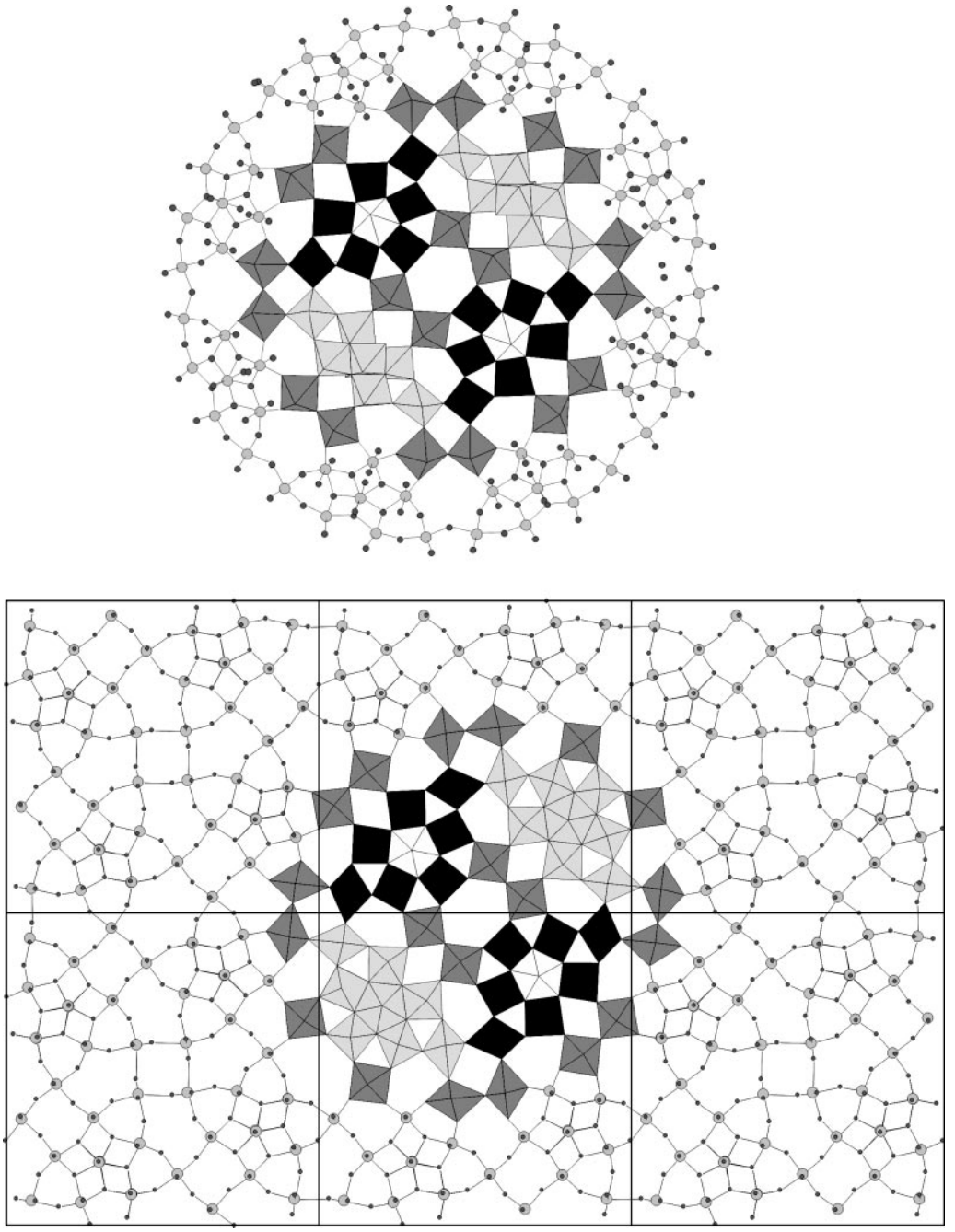

FIG. 13. Structural composition of the hubcap motif of the $\{Mo_{248}\}$ cluster and the related segment of the solid-state structure Mo_5O_{14}. Above: Schematic representation of one half of the $\{Mo_{248}\}$ cluster with a highlighted $\{36Mo\}$ hubcap. Below: Structure of Mo_5O_{14} viewed along the *c* axis. The hubcaps and the Mo_5O_{14} layer sections each contain four $\{Mo_8\}$ entities surrounding two central $\{Mo_2\}$ units. A central ring of six MoO_6 octahedra is formed by these two $\{Mo_2\}$ units and one MoO_6 octahedron of two opposite $\{Mo_8\}$ entities. Whereas in the case of the Mo_5O_{14} layer section the two remaining $\{Mo_8\}$ entities are of the type described above with one $\{Mo(Mo)_5\}$ pentagon which has two adjacent MoO_6 octahedra, in the case of the $\{Mo_{248}\}$ hubcaps two consist of an $\{Mo_6\}$ octahedron with two *trans*-positioned edge-sharing MoO_6 octahedra. The layers of the solid-state structure of Mo_5O_{14} can be formed approximately by formal superposition of the above-mentioned segment with 36 Mo centers.

assemblages approaching the limit of the macroscopic world (34, 35)? Dynamic light scattering experiments on solutions of the $\{Mo_{154}\}$-type clusters show, for instance, monodispersity with respect to the abundance of extremely large colloids with a hydrodynamic radius of ca. 40 nm (22), the structure of which is as yet unknown. Referring to biological systems we are dealing with a cluster size comparable to that of (spherical) viruses. Interestingly, surface

encapsulation with cationic long-chain surfactants allows the possibility of using these systems as precursors for materials in the electronics industry (36).

However, the nanosized polyoxomolybdate clusters now also provide model objects for studies on the initial nucleation steps of crystallization processes, an interesting aspect for solid-state chemists and physicists as the initial steps for crystal growth are not known. This is due to the fact that they represent well-defined molecular systems and have flexible (multidimensional) boundary conditions, i.e., clusters with circular and spherical topologies can be considered as potential precursors for such growth. It is envisaged that, with such an approach, it will be possible to unveil some of the mysteries associated with the biomineralization of structures such as the unicellular diatoms (37, 38). In the context of biomineralization, which takes place at room temperature (while chemists need high temperatures), it is remarkable that the linking of "giant-spherical" clusters to a well-defined solid-state layer structure is also possible at room temperature. In summary it is important in this context that (1) the aforementioned nanostructured building blocks can even be isolated (according to their stability) and (2) they have nanostructured cavities and well-defined properties, thus offering the possibility to construct materials with desired emergent properties using characteristic synthons, in accordance with the rule that the whole (due to cooperativity) is more than the sum of the parts.

ACKNOWLEDGMENTS

We are grateful to the Deutsche Forschungsgemeinschaft and the Fonds der Chemischen Industrie for financial support and L.C. thanks the Alexander von Humboldt Stiftung for a fellowship.

REFERENCES

1. K. A. Carrado and L. Q. Xu, *Micropor. Mesopor. Mater.* **27,** 87 (1999).
2. N. Papageorgiou, C. Barbe, and M. Grätzel, *J. Phys. Chem. B* **102,** 4156 (1998).
3. C. K. Loong, P. Thiyagarajan, J. W. Richardson, M. Ozawa, and S. Suzuki, *J. Catal.* **171,** 498 (1997).
4. T. R. Pauly, Y. Liu, T. J. Pinnavaia, S. Y. L. Bilinge, and T. P. Rieker, *J. Am. Chem. Soc.* **121,** 8835 (1999).
5. "Comprehensive Supramolecular Chemistry, Vol. 6, Solid-state Supramolecular Chemistry: Crystal Engineering," and "Vol. 7, Solid-state Supramolecular Chemistry: Two and Three-dimensional Inorganic Networks" (J. L. Atwood, J. E. D. Davies, D. D. MacNicol, F. Vögtle, and J. M. Lehn, Eds.), Pergamon/Elsevier, Oxford, 1996.
6. D. Voet and J. G. Voet, "Biochemistry," 2nd ed., p. 1076, Wiley, New York, 1995.
7. A. Müller, E. Krickemeyer, S. Dillinger, J. Meyer, H. Bögge, and A. Stammler, *Angew. Chem., Int. Ed. Engl.* **35,** 171 (1996).
8. (a) A Müller, F. Peters, M. T. Pope, and D. Gatteschi, *Chem. Rev.* **98,** 239 (1998); (b) A. Müller, P. Kögerler, and C. Kuhlmann, *Chem. Commun.* 1347 (1999).
9. M. T. Pope and A. Müller, *Angew. Chem., Int. Ed. Engl.* **30,** 34 (1991).
10. A. Müller, W. Plass, E. Krickemeyer, S. Dillinger, H. Bögge, A. Armatage, A. Proust, C. Beugholt, and U. Bergmann, *Angew. Chem., Int. Ed. Engl.* **33,** 849 (1994).
11. A. Müller, E. Krickemeyer, S. Dillinger, H. Bögge, W. Plass, A.Proust. D. Dloczik, C. Menke, J. Meyer, and R. Rohlfing, *Z. Anorg. Allg. Chem.* **620,** 599 (1994).
12. G. Huang, S. Zhang, and M. Shao, *Polyhedron* **12,** 2067 (1993) and references cited therein.
13. A. Müller, E. Krickemeyer, J. Meyer, H. Bögge, F. Peters, W. Plass, E. Diemann, S. Dillinger, F. Nonnenbruch, M. Randerath, and C. Menke, *Angew. Chem., Int. Ed. Engl.* **34,** 2122 (1995).
14. A. Müller, J. Meyer, E. Krickemeyer, and E. Diemann, *Angew. Chem., Int. Ed. Engl.* **35,** 1206 (1996).
15. A. Müller, E. Krickemeyer, H. Bögge, M. Schmidtmann, C. Beugholt, P. Kögerler, and C. Lu, *Angew. Chem., Int. Ed. Engl.* **37,** 1220 (1998).
16. (a) A. Müller, M. Koop, H. Bögge, M. Schmidtmann, and C. Beugholt, *Chem. Commun.* 1501 (1998); (b) A. Müller, E. Krickemeyer, S. Q. N. Shah, H. Bögge, M. Schmidtmann, and B. Hauptfleisch, *Inorg. Chem.*, in press; (c) M. J. Koop, Ph.D. Thesis, University of Bielefeld, Germany.
17. A. Müller, E. Krickemeyer, H. Bögge, M. Schmidtmann, and F. Peters, *Angew. Chem., Int. Ed. Engl.* **37,** 3360 (1998).
18. A. Müller, V. P. Fedin, C. Kuhlmann, H. Bögge, M. Schmidtmann, and F. Peters, *Chem. Commun.* 927 (1999).
19. A. Müller, S. Sarkar, S. Q. N. Shah, H. Bögge, M. Schmidtmann, Sh. Sarkar, P. Kögerler, B. Hauptfleisch, A. X. Trautwein, and V. Schünemann, *Angew. Chem., Int. Ed. Engl.* **38,** 3238 (1999).
20. A. Müller, S. Polarz, S. K. Das, E. Krickemeyer, H. Bögge, M. Schmidtmann, and B. Hauptfleisch, *Angew. Chem., Int. Ed. Engl.* **38,** 3241 (1999).
21. A. Müller, E. Krickemeyer, H. Bögge, M. Schmidtmann, C. Beugholt, S. K. Das, F. Peters, and C. Lu, *Chem. Eur. J.* **5,** 1496 (1999).
22. A. Müller and C. Serain, *Acc. Chem. Res.* **33,** 2 (2000)
23. L. Cronin, C. Beugholt, and A. Müller, *J. Mol. Struct.*, in press.
24. A. Müller and C. Beugholt, *Inorg. Chem.*, to be submitted.
25. A. Müller, C. Beugholt, M. Koop, S. K. Das, M. Schmidtmann, and H. Bögge, *Z. Anorg. Allg. Chem.* **625,** 1460 (1999).
26. A. Müller S. K. Das, V. P. Fedin, E. Krickemeyer, C. Beugholt, H. Bögge, M. Schmidtmann, and B. Hauptfleisch, *Z. Anorg. Allg. Chem.* **625,** 1187 (1999).
27. A. Müller, S. K. Das, H. Bögge, C. Beugholt, and M. Schmidtmann, *Chem. Commun.* 1035 (1999).
28. A. Müller, E. Krickemeyer, H. Bögge, M. Schmidtmann, F. Peters, C. Menke, and J. Meyer, *Angew. Chem., Int. Ed. Engl.* **36,** 484 (1997).
29. S. W. Zhang, Y. G. Wei, Q. Yu, M. C. Shao, and Y. Q. Tang, *J. Am. Chem. Soc.* **119,** 6440 (1997).
30. G. Liu, Y. G. Wei, Q. Yu, Q. Liu, and S. W. Zhang, *Inorg. Chem. Commun.* **2,** 434 (1999).
31. A. Müller, S. Q. N. Shah, H. Bögge, and M. Schmidtmann, *Nature* **397,** 48 (1999).
32. P. Ball, *Nature* **395,** 745 (1998).
33. (a) F. A. Colton and G. Wilkinson, "Advanced inorganic chemistry," 4th ed, p. 847, Wiley, New York, 1980; (b) A. Müller, and B. Hauptfleisch, in preparation.
34. A. Müller, *J. Mol. Struct.* **325,** 13 (1994).
35. A. Müller and M. T. Pope, *in* "From Simplicity to Complexity, Part II, Information–Interaction–Emergence," K. Mainzer, A. Müller, and W. G. Saltzer (eds.), p. 57, Vieweg, Wiesbaden, 1998.
36. A. Müller, and D. Volkmer, personal communication, 1999.
37. A. M. Schmid, R. K. Eberwein, and M. Hesse, *Protoplasma* **193,** 144 (1996).
38. R. Gordon and R. W. Drum, *Int. Rev. Cytol.* **150,** 243 (1994).